

Synergistic Fabrication of Dose–Response Chitosan/Dextran/ β -Glycerophosphate Injectable Hydrogel as Cell Delivery Carrier for Cardiac Healing After Acute Myocardial Infarction

Dose-Response:
An International Journal
July-September 2020:1-10
© The Author(s) 2020
Article reuse guidelines:
sagepub.com/journals-permissions
DOI: 10.1177/1559325820941323
journals.sagepub.com/home/dos



Chongjun Hua¹, Jing Liu², Xiuhong Hua³, and Xinyu Wang⁴

Abstract

The human mesenchymal stem cells (hMSCs) therapy offering an encouraging the new methods to establish the conveying on the chitosan (C)/dextran (D)/ β -glycerophosphate (β -GP) loaded with hMSCs to enhance the acute myocardial infarctions. The synthesized hMSCs-CD@ β -GP system displayed the ratio of determination modules, size of the pore, absorbency, and the swellings ratio in the assortment of the 65 ka, $149 \pm 39.8 \mu\text{m}$, 92.2%, 42 ± 1.38 , and 29 ± 1.9 , respectively. The fabricated hMSCs-CD@ β -GP was highly stable and physicochemical investigated and confirmed the suitability of the materials for cardiac regeneration applications. The in vitro examinations of the injectable hydrogels with hMSCs-CD@ β -GP have recognized that the improved survival rate of the cells, increased the pro-inflammatory expressions factors, pro-angiogenic factors analysis confirmed the promising results of the ejection of fractions, fibrosis area, vessel density with decreased infarctions size, with suggesting that the remarkable improvement of the heart regenerative function after myocardial infarctions. The new synergistic approach of the injectable hydrogels with hMSCs could able appropriate for the effective treatment of cardiac therapies after acute myocardial infarctions.

Keywords

chitosan/dextran/ β -glycerophosphate composition, dose–response injectable hydrogels, mesenchymal-derived stem cells, myocardial infarctions

Introduction

Acute myocardial infarction (AMI) is one of the serious concerns of cardiovascular diseases which occurs by the lack of prolonged supply of oxygen and nutrients that limits the heart's capacity of anaerobic metabolism in the heart muscles. Heart failure, impulsive death, privation of left ventricular function, and ischemic heart diseases are the highly complicated exposure arrived by AMI.¹⁻⁴ Additionally, disruption of homeostatic balance causes series of successive events like ventricular stiffness, inflammatory effects, necrosis, apoptosis, remodeling that leads to forming scar and altered contractility in heart muscles. Surgical and medical approaches like percutaneous coronary intervention and pharmacotherapies can significantly enroll their contribution toward appalling effects of AMI.⁵⁻⁷ However, they exhibit impotent toward regenerating myocardium and constructing new contractile tissues. Regarding to

overcome this problem, experimentally and practically significant risk heart transplantation is only obligatory treatment for AMI. Hence, in point of avoiding this complicate treatment,

¹ Department of Cardiology, Jinhua Central Hospital, Jinhua, China

² Department of Cardiology, Yantai Affiliated Hospital of Binzhou Medical University, Yantai, China

³ Department of Pharmacy, Jinhua Fifth Hospital, Jinhua, China

⁴ Department of Ultrasonography, Xiamen Cardiovascular Hospital Xiamen University, Xiamen, China

Received 22 April 2020; received revised 26 May 2020; accepted 1 June 2020

Corresponding Author:

Xinyu Wang, Department of Ultrasonography, Xiamen Cardiovascular Hospital Xiamen University, No. 2999, Jinshan Road, Huli District, Xiamen-361006, China.

Email: wxinyu38@yahoo.com



Creative Commons Non Commercial CC BY-NC: This article is distributed under the terms of the Creative Commons Attribution-NonCommercial 4.0 License (<https://creativecommons.org/licenses/by-nc/4.0/>) which permits non-commercial use, reproduction and distribution of the work without further permission provided the original work is attributed as specified on the SAGE and Open Access pages (<https://us.sagepub.com/en-us/nam/open-access-at-sage>).

novel recognition of researchers has led to the ideology of cell transplantation, an emerging therapeutic strategy against AMI.⁸⁻¹⁰

In the field of tissue engineering applications, hydrogels play an important role. The hydrogels show a local tissue environment to forms significant efforts to forming biological and biochemical new functions.¹¹⁻¹³ The hydrogels involved the formation of polymeric, ceramic, nanotubes, graphene, and metallic nanostructures. Accordingly, the hydrogels are used for the cell encapsulation, transplantation, and various fields for the tissue application process, for intense the cells reorganized ligand exchange for the cellular matrix to interacts the cellular membrane proteins in the forms of various cell types.¹⁴⁻¹⁷ The collagen fibrils in the tissue engineering hydrogels of alginate and collagen can deliver the adhesion spot of the cell adhesion. Also the alginate hydrogels lack the ranked the fibril structure of local tissues. The native collagen binding the target binding of the Arg-Gly-Asp binding peptide site in the cell adhesion process. Lastly, collagen holds the typical nanotopography piece, indifference to the same.¹⁸⁻²⁰

Cells from various sources of human like cardiac stem cells, bone marrow stem cells, mesenchymal stem cells, hemotoprostic stem cells, embryonic stem cells and so on have exploited for the purpose of regenerative myocardium tissues. Even though cell therapies made by different forms of cells have been favorable to improve the function of cardiac, they are not the real accepted occupier of heart tissues. Additionally, studies on stem cells apart from cardiac stem cells reported certain disadvantages like inconsistent efficacy, no effect in reducing scar size and shrinkage of scar tissue.²¹⁻²³ Though the cell therapy composed by various forms of cells has been favorable to enhance the functions of cardiac, they are an acceptable specific resident of the cardiac tissue.²⁴ Besides, there are several reports are depicted the stem cells derived from the cardiac tissues with reducing less scar sizes and scar shrinkages of the tissues. The cardiac cells have persuasive propertied such as the production of endothelial, smooth muscles cells, and angiogenesis cells. Even though, the stem cells are features of distinguishable toward the immuno-modulation and immuno-suppression properties.²⁵⁻²⁸

Synergic methods, as well, a promising strategy and biocompatible, biodegradable materials are required for efficient cardiac stem cells transplantation to associate the treatment for AMI. Hence, a pouch-like hydrogel materials like collagen, gelatin, and fibroin can serve as a potential and medically advantageous candidate in drug delivery systems, cell therapy, creation and regeneration of muscle tissues, and controlled release of systems.²⁹⁻³² Nowadays, hydrogel materials are widely used in biomedical and pharmaceutical field for its distinct properties like biocompatible, biodegradable, swelling ability, and non-toxicity. Combination of biopolymers like chitosan (C), with hydrogel has been demonstrated as an efficient candidate for stem cell transplantation. Also C is a trademark example for its excellent biocompatible, biodegradable,

antimicrobial, immunostimulatory activities.^{33,34} Materials fabricated with C have been widely reported and investigated in medical field such as drug release, tissue engineering, catalysts and enzyme carrier, medical implantation, wound healing, and also in other fields such as recovery of metal ions, energy storage, protective clothing materials, biosensors, and energy storage. In recently, Chen et al,³⁵ developed the engineered by mimic micro RNA (miRNA)-21 was deliver as promising nanoparticle approaches of the nucleic acids mediated via calcium ions bridge.^{36,37}

Taking to the advantages, we have described on the delivery of human mesenchymal stem cells (hMSCs) utilizing C /dextran (D)/ β -glycerophosphate (β -GP) hydrogel composition for myocardial infarctions. We found that the injectable hydrogel with additions of various formulations at room temperature (RT) displayed excellent promising mechanical strength and gelation time for the cell proliferation. These properties may generate this injectable hydrogel as potential cell delivery of the cell engraftment for the myocardial infarctions treatment (Figure 1). This injectable hMSCs-CD@ β -GP system could facilitate the angiogenic gene to the cardiac tissues to protect the beating heart damages.

Methods and Materials

Characterization Techniques

The gelation time of the injectable hydrogels was examined by the vial invention analysis.³⁸⁻⁴⁰ The starting solutions of C, D, and β -GP were immersed at RT. The gelation time was examined via inverting the immersed solutions and monitoring the flow ratio. All the gel times were repeated 3 times for every groups. The hydrogel morphology was examined via scanning electron microscopy (Hitachi S4800), and the porous size of the hydrogel was analyzed by the IP6 software's. The hydrogels were lyophilized and freeze-dried and sputter-coatings with gold at 20 mA for 60 seconds priors to SEM examinations.

Fabrication of C@ β -GP and CD@ β -GP Injectable Hydrogel

The hydrogel preparation was fabricated by the previously reported methods.⁴¹⁻⁴³ In this examination, the 3 components of the CD@ β -GP hydrogels as below. The C solution was synthesized by the dissolving of C (150 mg) in 7 mL acetic acid solution under RT. The solution was separated and undissolved particles removed at the least concentrations of C can be calculated to be 1.80%. Further, the β -GP was synthesized as an aqueous solution (50%) preserved at 5 °C for the above method. Various concentrations of D (0.5%, 1.0%, 1.5%, 2%) were immersed then added to the synthesized C solution. Then, the β -GP solution was added dropwise in the same solution and the solution stirring at 10 minutes to become saturated solutions. Lastly, the formulation of CD@ β -GP injectable hydrogel

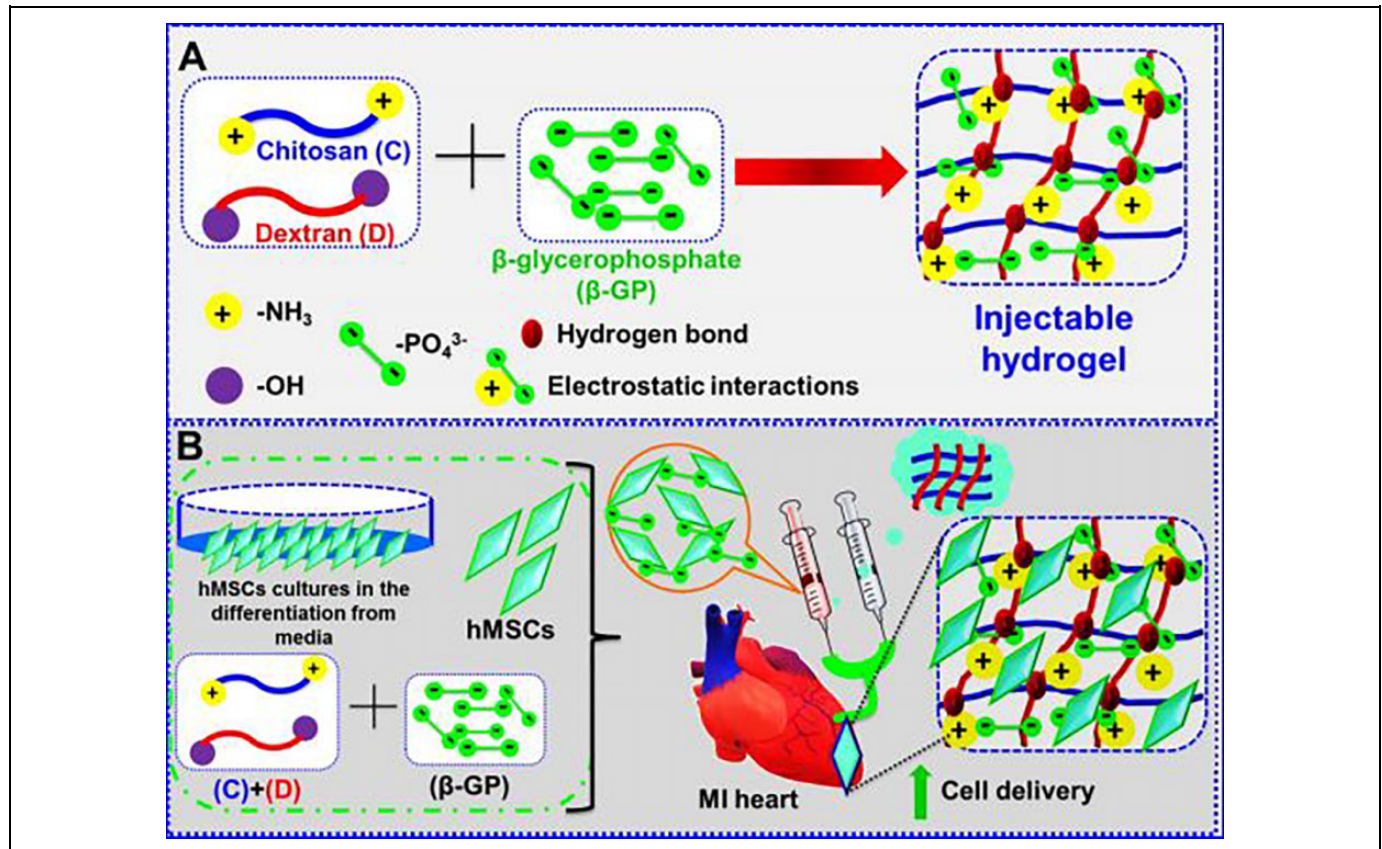


Figure 1. A, Fabrication method of CD@ β -GP injectable hydrogel. B, Human mesenchymal stem cells encapsulated in hydrogels can be utilized in cardiac repair application after myocardial infarctions. C indicates chitosan; D, dextran; β -GP, β -glycerophosphate.

was synthesized by the gel reaction solution at room temperature. The CD@ β -GP injectable hydrogel and without D was used a positive control of the work.

Enzymatic Degradation Properties of Injectable Hydrogels

The swelling of hydrogels vital role of the moieties design. The porous of the crosslinker pores the exact delivery vehicle and gases and nutrients for specific cell survival.⁴⁴⁻⁴⁶ We examined the selling of the hydrogenation moieties. The increasing porous size could accredit to the enlarged permeability of frameworks after the combination of CD@ β -GP. The biodegradability of the hydrogels was monitored by enzymatic degradation examinations in vitro. All the hydrogels were startlingly freezing and weighted before the investigations. The hydrogel was dissolved in phosphate buffered saline (PBS; 20 mL and 7.4 pH) featuring either 0% or 3% lysozyme at RT with a 50 RPM string rate for 4 weeks. The PBS was changed every week. A sudden time point, the degraded injectable hydrogels were washed and freeze-dried and the weights were recorded. The degradation percentage was investigated by the previously reported methods.

Isolation of Mesenchymal-Derived Stem Cells

Human mesenchymal stem cells were isolated from female Wister rats weighing about 250 g with 20 to 23 weeks of age. Initially, the atrial samples of rats were collected and cut into small pieces followed by suspension in F12K medium ref. which also contains collagenase (1-3 mg/mL). Then, the cells were plated in Petri dishes with excess of F12 medium mixed with 10% fetal bovine serum, recombinant human fibroblast (100 mg/mL), L-glutathione in minimal amounts, and human erythropoietin (10 μ g/mL). After 8 to 10 days of incubation this cultured plates, cells maintained and expanded mostly c-kit CSCs. Expanded cells were allowed for immunomagnetic separation with microbeads to obtain c-kit CSCs.⁴⁷⁻⁴⁹

Animal Model and Experimental Groups for MI

The animals care and experimental protocol were utilizing though the strategies by the animal care unit of the department of ultrasonography, cardiovascular Hospital of Xiamen University, Xiamen, China. Induction of MI was performed to the procedure according to the authorized literature procedure. Ten Male Fischer rats with the age of about 5 to 7 weeks and weighing about 250 to 300 g were acquired from Chinese Medical University and housed 3 per cage, maintained at RT and atmospheric conditions. Ad libitum food and water were

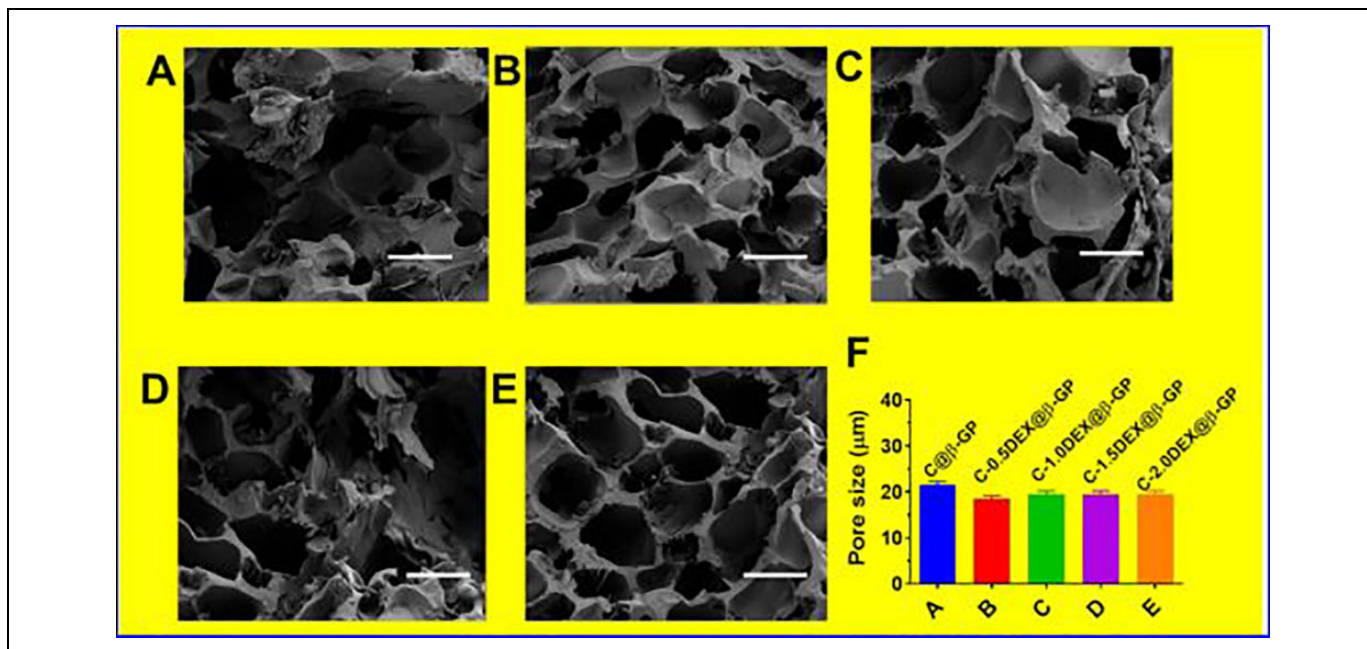


Figure 2. Temperature response of the chitosan and dextran (0.5%, 1%, 1.5%, and 2% of dextran) incorporation with CD@β-GP injectable hydrogel (A-E) SEM images of different hydrogel groups; scale bar 200 μm; (F) pore size of various hydrogel groups; (D) the pore size of various hydrogel groups. C, chitosan; D, dextran; β-GP, β-glycerophosphate.

provided for the rats and experiment was started after animals become comfortable for the new environment. Separation of animals groups into 4 groups have carried out randomly with each group carries 4 animals. All the groups were subjected for the induction of MI as reported in literature. Group I-untreated (used a healthy animal). Group II was injected by the free hMSCs-CD@β-GP (0.5 μg/μL) with saline through the 30-mm needle syringe. Group III was injected by the hMSCs-CD@β-GP (0.5 μg/μL), group IV was injected by the hMSCs (5×10^5 cells in 100-μL saline by the injection of the HMSCs). The preparation and identification of the samples were successfully injecting with infarcted diets through the bleb over the infarct place. The rats were examined every 3 days of climate-controlled and sterile rooms with easy access to food.

Statistical Analysis

All data are presented as the mean \pm SD. Significant differences between groups were analyzed by Student *t* test (2 groups), 1-way analysis of variance (ANOVA; multiple groups), or 2-way repeated ANOVA, and $P \leq .05$ was considered significantly different. Statistical analyses were performed with GraphPad Prism version 9.0 (GraphPad Software).

Results and Discussion

Synthesis and Characterization Methods of hMSCs-CD@β-GP Hydrogels

The graphical representation and possible methods of fabrication of CD@β-GP injectable hydrogel shown in Figure 1A. The

electrostatic interactions between the positive charge ammonium segment groups resided on the C chains. Though, the interaction repulsions were reduced by the addition of β-GP due to the negatively charged fragments. So, the glycerol segment of the β-GP could interact with water moiety and enhance the hydrogelation of C groups and retain in a polymeric chain stretched free in aqueous solutions. The internal energy enhanced with the increasing temperature and the break the hydrogen bond between C groups. After the water moiety release from the C groups. Additionally, enhance of temperature electrostatic interaction between the polymers leads to the improvement of ionic strengths and mores polymeric hydrophobic interactions, suggesting the formation of the injectable hydrogels.

The hydrogel solutions were acquired after the fabrication of C, D, and β-GP solution and flowed at RT. The solutions turn into the electrostatic interaction and bonding between the hydrogen of C, D, and β-GP (Figure 1A). By adding 0.5%, 1%, 1.5%, and 2% of D, it found that gelation times of the samples of CD@β-GP were about 20-fold lesser than the C@β-GP hydrogels due to the bonding interactions between the hydrogen of phosphate groups on β-GP. The SEM image shows that the hydrogels having clear porous structures with exact formations like sheet morphologies. Also, we further examine the morphologies of hydrogels with CD@β-GP, and it displays the hydrogels having highly porous (Figure 2A-E). The porosity of the hydrogels increases the C and D (0.5%, 1%, 1.5%, and 2% of D) and incorporation with CD@β-GP models was 85%. The exact porous size of the β-GP moieties was in the range between 150 and 200 μm (Figure 2F). This porous size is exactly suitable for the incorporation with

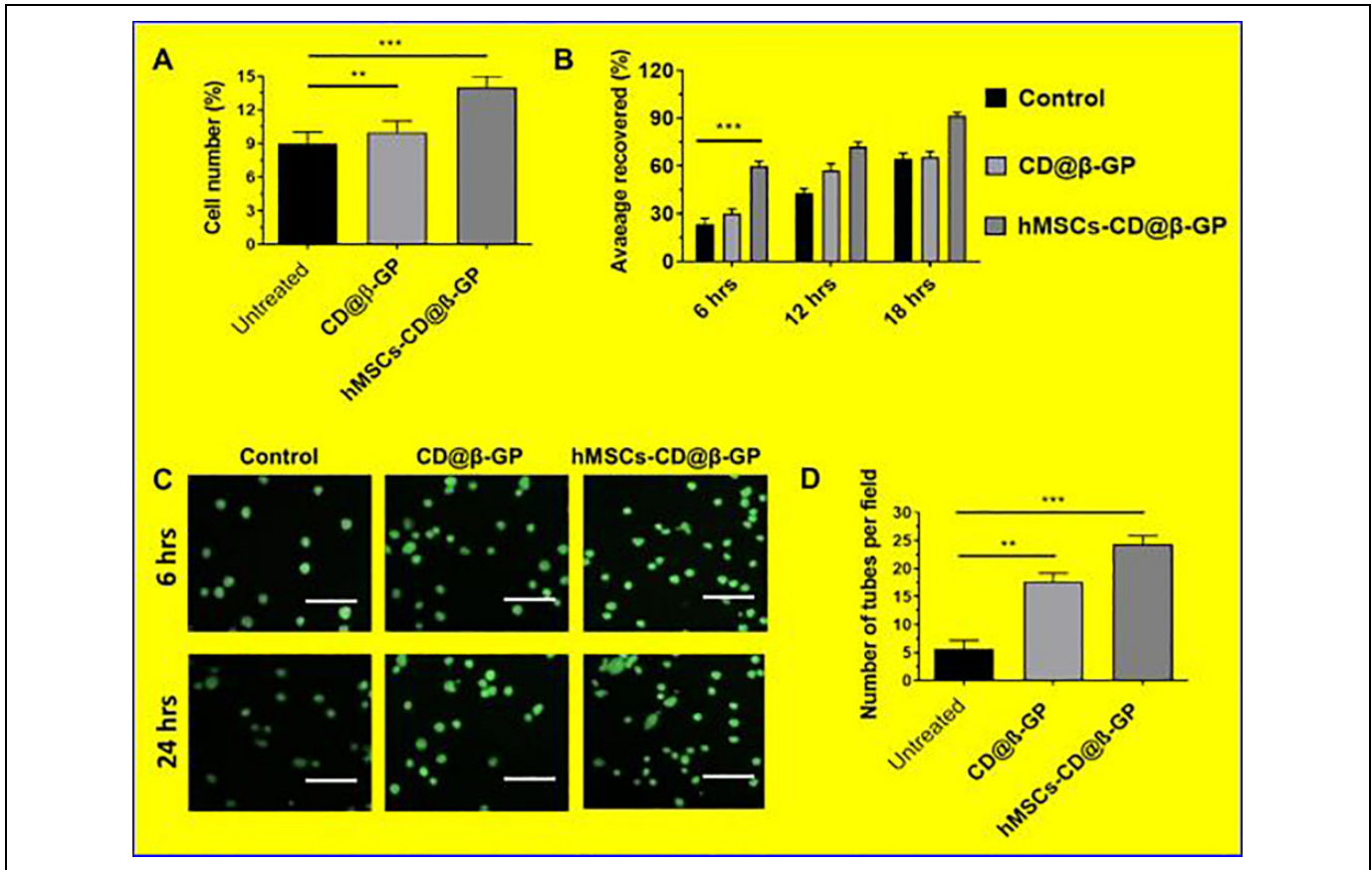


Figure 3. The cell compatibility and angiogenic potential of hMSCs with prepared hydrogels in vitro. A, The MTT assay of the hMSCs in vitro quantitative analysis cell proliferation. B, Quantitative analysis of area covered (cell migrations) by hMSCs in various periods (6, 12, and 18 hours). C, Microscopic evaluation of cell proliferation and tube formations with prepared hydrogel medium after 24 hours of incubation. D, The tube formation quantitative determinations after 24 hours. hMSCs indicates human mesenchymal stem cells.

fibroblast, endothelial, and stem cells. The density model of the hydrogels was gotten in both dry and wet conditions, and it was detected that the adding of CD@β-GP had prompted in a decrease in the density model (Figure 1B). This might be due to an increase in porous by 5%. The model of C and D segments in wet ailment was 72 kPa though that of CD@β-GP was 65 kPa. These parameters are very close to the extensive models' values that were previously described for the tissue regenerations.

Enzymatic Degradation Properties of Injectable Hydrogels

The degradation of the polymeric compounds is important to the biological process due to the direct relation to the human lives. The weights of injectable hydrogels were gradually reduced with the incubation periods. The quick degradation at the initial stage was caused by the β-GP because it was free from the hydrogels and forms the hydrogels insufficient cross-linkers. Then, the degradation ratio was reduced and hydrogels were displayed improved anti-hydrolysis behaviors with a high degradation ratio of 70% for up to 4 weeks. In contrast to the C@β-GP, the different

ratio hydrogels C-(1.0 D)@β-GP displayed a less weight loss ratio, which may be due to the improved hydrogen bond interactions formation with D. The same trend of hydrogel degradation also depicted in lysosomes environments. The hydrogel was quickly degraded when the samples in lysosomes solutions. This may be due to the C and D chain was decomposed via lysosomes. These outcomes suggested that the C-(1.0 D)@β-GP hydrogels demonstrated a stable and high degradation ratio for 4 weeks, and this may will deliver the promising possessions for its application in vivo.⁵⁰⁻⁵²

The biocompatibility and suitability of the fabricated hydrogel matrixes were examined via in vitro methods. The in vitro cell viability and cell proliferations were investigated by using human coronary artery endothelial cells (HCAECs) cultured on the prepared hMSCs-CD@β-GP and the values were quantitatively measured as exhibited in Figure 3. It is well-known that C and D chain hydrogels have significantly favorable for the cell proliferations. These presented results demonstrated that CD@β-GP hydrogel reliably had significant survival rate and proliferation percentage compared to the bare CD@β-GP hydrogel matrixes. The cell proliferations have no significant effect on 6 hours and 12 hours for the hydrogels. Nonetheless,

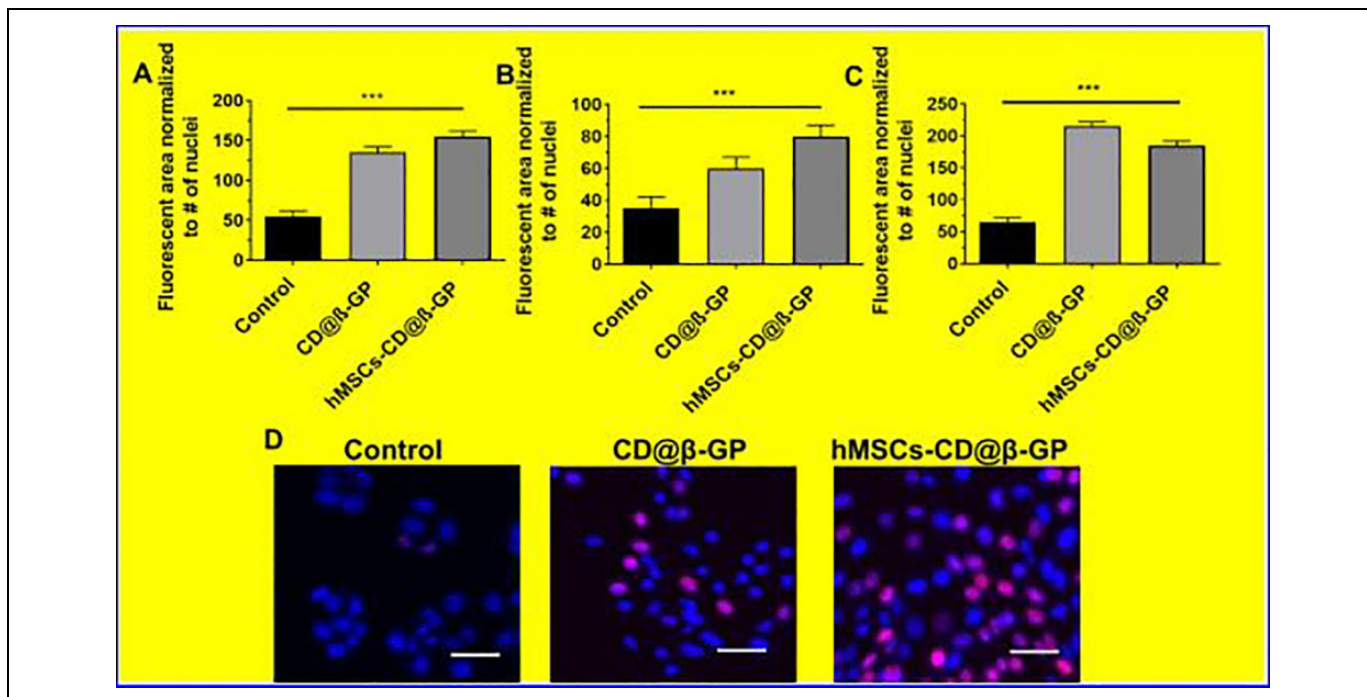


Figure 4. A-C, The cardio markers expression early stage in vitro treated with CD@ β-GP and hMSCs-CD@β-GP. D, The fluorescence microscopic examination of GS@L and hMSCs-CD@β-GP. Scale bar μm. C indicates chitosan; D, dextran; hMSCs, human mesenchymal stem cells; β-GP, β-glycerophosphate.

on 18 hours, the proliferation percentages have increased significantly on the CD@β-GP hydrogel sample.

In addition, we have investigated cardiomyocytes proliferation ability of the hydrogels were preliminary investigated by using early cardiac transcription factors with cardiomyocyte progenitor (hCMPs) cells. The cultured samples of CD@β-GP hydrogel have a significant enhancement in the selected early cardiac markers (SAC, Cx43, and cTnI) after 5 days of culture. These results suggest that CD@β-GP hydrogel have favorable cardiac progenitors and cardiomyocytes mitotic activity as exhibited in Figure 4. Hence, we could preliminary confirm the prepared hydrogel can be suitable for in vivo proliferation and differentiation of cardiomyocytes in cardiac regeneration.

The hemodynamic examinations of saline and hydrogel-treated groups were measured. No significant body weight and heart rate differences were observed between the hydrogel groups in the presence and absence of hMSCs 4 weeks post-treatment. The hMSCs-CD@β-GP hydrogel group and control sample have enhanced cardiac output, contractility index, and left ventricle (LV) pressure when associated to the CD@β-GP hydrogel and saline-treated groups. The preliminary in vivo cytocompatibility of the hydrogel samples were examined to confirm no significant immune response against model animals. The resulting studies of immuno-histochemical staining on myocardial tissues demonstrated that there is no significant damages of cardiomyocytes and inflammation factors (tumor necrosis factor [TNF-α]) after hMSCs-CD@β-GP and CD@β-GP injection as shown in Figure 5. In addition, there was no

significant differences of pro-inflammatory factors (TNF-α and miR-146) and cardiomyocyte apoptotic gene (miR-145 and cyclin D1) and miRNA expressions in hydrogel samples when compared to the control (Figure 5). Therefore, we could be concluded that the prepared hydrogel samples are greatly compatible for the cardiac regeneration applications.

In order to examine the action of hMSCs encapsulated CD@β-GP injectable on the post-MI cardiac functions after intramyocardial injection to the model animal myocardial infarction models. The cardiac function of infarcted model before and after hMSCs-CD@β-GP hydrogels and control was evaluated by the echocardiographic techniques as exhibited in Figure 6. The results of echocardiography were established that hMSCs encapsulated CD@β-GP injected MI group have significantly reduced the LV remodeling 30 posttreatment, which is very important to avert heart failures through MI. The ejection fraction (EF; 78.56 ± 5.45) and fractional area change (FA; 58.34 ± 3.5) were substantial improvement in the hMSCs-CD@β-GP encapsulated hydrogels when compared to the CD@β-GP injectable hydrogel and saline group. In mean time, CD@β-GP injectable hydrogel group also have reasonable improvement of EF and FA change, due to its active functional groups structure and biocompatible activity. The left ventricle internal dimensions of hydrogel-treated group during diastole and systole were 6.43 ± 0.50 mm and 4.45 ± 0.25 mm, respectively, which improved values when compared to the CD@β-GP injectable hydrogel- and saline-treated group. And hMSCs-CD@β-GP hydrogel-treated group also have improved values of end-systolic and end-diastolic volumes

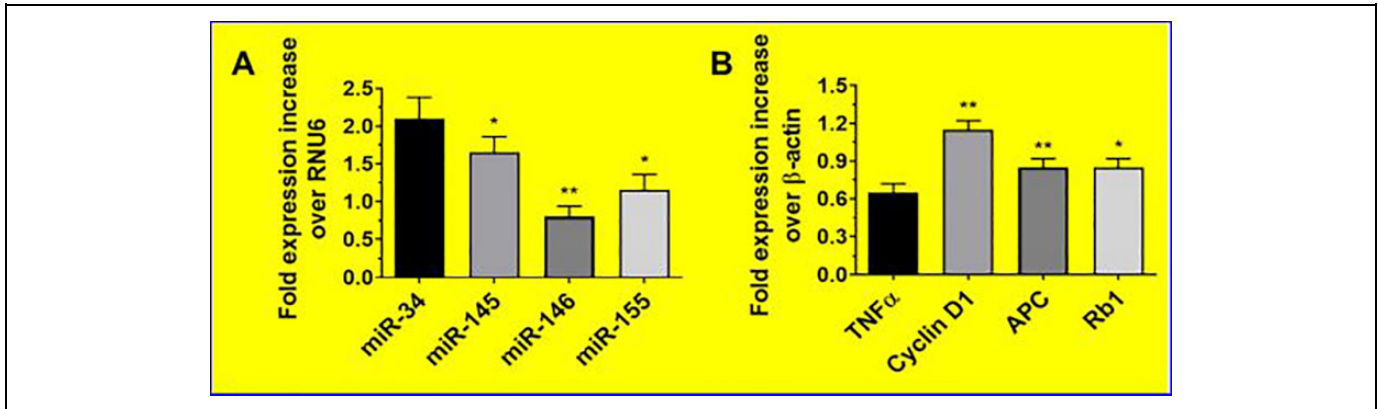


Figure 5. The gene expression level of the cardio stress and inflammatory markers genes examined by qPCR analysis. qPCR indicates quantitative polymerase chain reaction. * $p < 0.05$. ** $p < 0.01$.

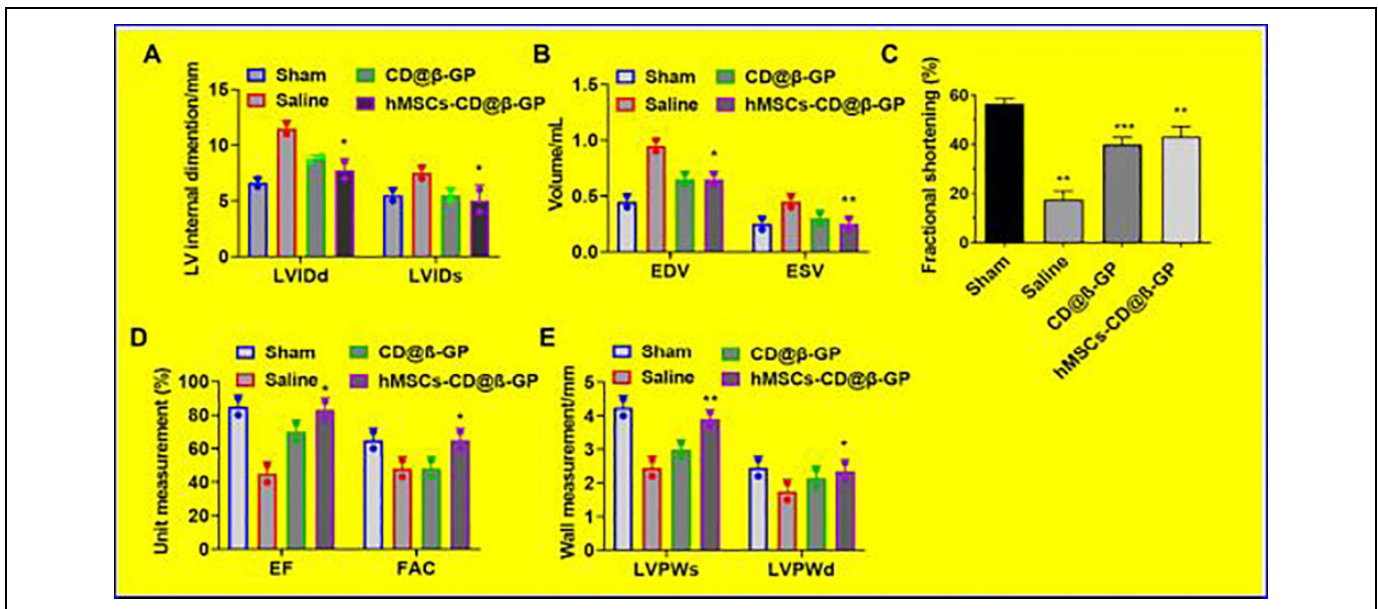


Figure 6. In vivo cardiac remodeling echocardiography analysis after injection of the CD@ β -GP and hMSCs-CD@ β -GP at 28 days post-administration. A, Left ventricular internal dimensions of systole and diastole (LVIDs and LVIDd). B, End systolic and diastolic volume (ESV and EDV) measurement. C, Fractional shortening. D, Determinations of ejection fraction and fractional area change and left ventricular posterior wall at systolic and diastolic sites. C indicates chitosan; D, dextran; hMSCs, human mesenchymal stem cells; β -GP, β -glycerophosphate. * $p < 0.05$. ** $p < 0.01$. *** $p < 0.001$.

such as 0.22 ± 0.05 and 0.59 ± 0.04 mL, respectively, confirming the operative cardiac functioning of hydrogel samples (Figure 6). The wall measurement of left ventricular posterior at systole and diastole has improved greatly after hydrogels-treated groups in the presence and absence of hMSCs-CD@ β -GP compared to the saline treated groups. From those observations, we can be confirming that hMSCs-CD@ β -GP encapsulated hydrogel sample have greater cardiac performances as well as CD@ β -GP injectable hydrogel without hMSCs-CD@ β -GP also provide a reasonable cardiac function, due to its biocompatibility and presence of chemically active groups.

The infarctions area and size of the treatment group was semi-quantitatively investigated by the cross sections of middle

papillary muscles 28 days postadministrations. Subsequently, the developed survival of cardiomyocyte in the periinfarct part was shown in the hMSCs-CD@ β -GP hydrogel- and control-treated groups succeeding enhanced wall width associated with the saline treatment group. So, the importantly growing angiogenesis and reducing cardiomyocytes necrosis of hydrogels treatment acute-infarcted area have been significantly related with the improvement of cardiac purposes in MIs models (Figure 7). The myocardial infarctions treatment with mesenchymal-derived stem cell therapy recently developed with the researchers, yet still, to date there are various problems to convey the mesenchymal stem cell at infarcted heart tissues. The present examination established that the robust hydrogels

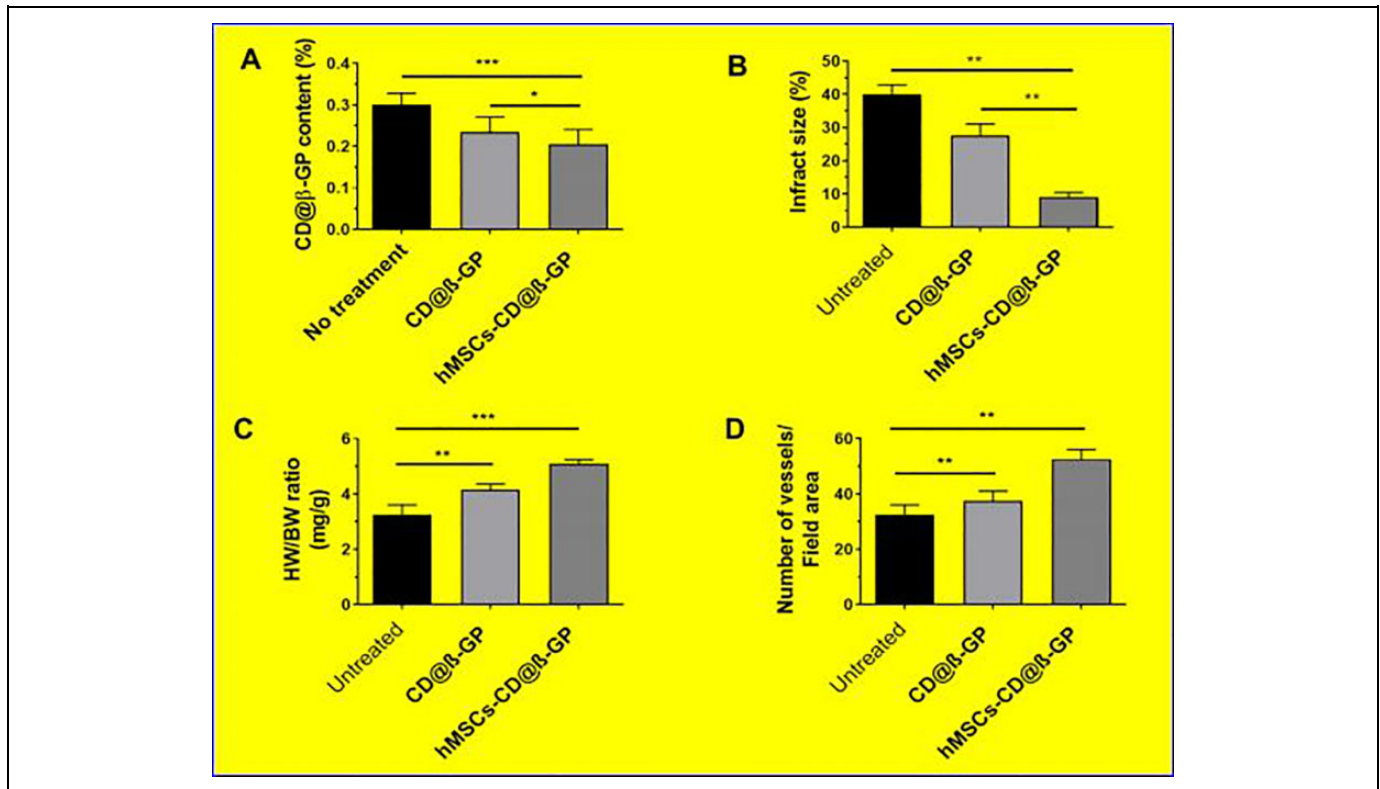


Figure 7. A, CD@β-GP content of infarcted regions after hydrogel treatment. B, Measurement of infarcted area reduction. C, Determinations of ratio between heart weight to body weight after treatment and (D) quantitative analysis data of vessels. C indicates chitosan; D, dextran; β-GP, β-glycerophosphate.

with different mesenchymal stem cells have remarkable effects on the cardiac regenerations and infarctions.

Conclusion

The simplistic easily injectable hydrogels encapsulated with hMSCs were established significantly to the cardiac remodeling after acute AMI. The injectable hydrogels of C@β-GP and CD (0.5-2%)@β-GP were successfully synthesized via electrostatic interactions and hydrophobic attractions. The injectable hydrogels have displayed excellent gelation time and biodegradations property. Our present work demonstrates that the C@β-GP and CD(0.5-2%)@β-GP hydrogels depicted that remarkable cell viability and proliferation of the HCAECs cells in vitro. The hMSCs encapsulated hydrogels were effectively injected into the myocardial infarcted region of in vivo animal model examinations, achieving a noticeable action for the cardiac renewal with improved activities of vessel densities, EFs with abridged infarcted size of the AMI heart sites. The inspective outcomes suggest a new strategy of cardiac transplant resources and a novel opportunity of cardiac remodeling therapeutics method after AMIs.


Declaration of Conflicting Interests

The author(s) declared no potential conflicts of interest with respect to the research, authorship, and/or publication of this article.

Funding

The author(s) received no financial support for the research, authorship, and/or publication of this article.

ORCID iD

Xinyu Wang  <https://orcid.org/0000-0003-1881-5200>

References

1. Prabhu NV, Maiya AG, Prabhu N. Impact of cardiac rehabilitation on functional capacity and physical activity after coronary revascularization: a scientific review. *Cardiol Res Pract.* 2020; 2020:1236968. doi:10.1155/2020/1236968
2. Wilson AS, Watts JA, Bush KNV. Active duty personnel with ST elevation myocardial infarctions are deployment ineligible despite receiving standard management. *Mil Med.* 2020;185(5-6):e638-e642. doi:10.1093/milmed/usaa026
3. Ruzsa Z, Januszek R, Óriás V., et al. Mortality and chronic obstructive pulmonary disease in patients treated with endovascular revascularization of the infra-inguinal lower limb arteries from retrograde access. *Ann Translational Med.* 2020;8(5):206. doi:10.21037/atm.2020.01.57
4. Andrabi T, French KE, Qazilbash MH. New cancer therapies: implications for the perioperative period. *Curr Anesthesiol Rep.* 2018;8(5):362-367. doi:10.1007/s40140-018-0303-4

5. Ojha N, Dharmoon AS. *Myocardial Infarction*. StatPearls Publishing, Treasure Island (FL); 2019. Accessed February 7, 2019. <http://europepmc.org/abstract/MED/30725761>.
6. Marchand DK, Farrah K. *Thrombolytics for Acute Myocardial Infarction in a Prehospital Setting: a Review of Comparative Safety, and Guidelines*. Canadian Agency for Drugs and Technologies in Health; 2019. Accessed July 9, 2019. <http://europepmc.org/abstract/MED/31525008>.
7. Rehani PR, Ifikhar H, Nakajima M, Tanaka T, Jabbar Z, Rehani RN. Safety and mode of action of diabetes medications in comparison with 5-aminolevulinic acid (5-ALA). *J Diabetes Res*. 2019;2019:4267357. doi:10.1155/2019/4267357
8. Dhama K, Latheef SK, Dadar M, et al. Biomarkers in stress related diseases/disorders: diagnostic, prognostic, and therapeutic values. *Front Mol Biosci*. 2019;6:91. doi:10.3389/fmolb.2019.00091
9. Shiomi M. The History of the WHHL rabbit, an animal model of familial hypercholesterolemia (i)—contribution to the elucidation of the pathophysiology of human hypercholesterolemia and coronary heart disease. *J Atheroscler Thromb*. 2020;27(2):105-118. doi:10.5551/jat.RV17038-1
10. Smit M, Coetzee AR, Lochner A. The pathophysiology of myocardial ischemia and perioperative myocardial infarction. *J Cardiothorac Vasc Anesth*. 2019:S1053–S1077(19)31038-31039. doi:10.1053/j.jvca.2019.10.005
11. Popa MO, Irimia MN, Papageorghe MN, et al. The mechanisms, diagnosis and management of mitral regurgitation in mitral valve prolapse and hypertrophic cardiomyopathy. *Discoveries*. 2016; 4(2):e61. doi:10.15190/d.2016.8
12. Liao X, Yang X, Deng H, et al. Injectable hydrogel-based nanocomposites for cardiovascular diseases. *Front Bioeng Biotechnol*. 2020;8:251. doi:10.3389/fbioe.2020.00251
13. Jin M, Wang Y, Wang Y, et al. Protective effects on corneal endothelium during intracameral irrigation using N-(2)-l-alanyl-l-glutamine. *Front Pharmacol*. 2020;11(2020):369. doi:10.3389/fphar.2020.00369
14. Park BW, Jung SH, Das S, et al. *In vivo* priming of human mesenchymal stem cells with hepatocyte growth factor-engineered mesenchymal stem cells promotes therapeutic potential for cardiac repair. *Sci Adv*. 2020;6(13):eaay6994. doi:10.1126/sciadv.aay6994
15. Zhou X, Jin N, Wang F, Chen B. Mesenchymal stem cells: a promising way in therapies of graft-versus-host disease. *Cancer Cell Int*. 2020;20:114. doi:10.1186/s12935-020-01193-z
16. Yeung V, Willis GR, Taglauer E, Mitsialis SA, Kourembanas S. Paving the road for mesenchymal stem cell-derived exosome therapy in bronchopulmonary dysplasia and pulmonary hypertension. *Stem Cell-Based Therapy for Lung Disease*. (n.d.). 2019: 131-152. doi:10.1007/978-3-030-29403-8_8
17. Nordio G, Bustin A, Odille F, et al. Faster 3D saturation-recovery based myocardial T1 mapping using a reduced number of saturation points and denoising. *PLoS One*. 2020;15(4):e0221071. doi: 10.1371/journal.pone.0221071
18. Kagiya N, Shrestha S, Cho JS, et al. A low-cost texture-based pipeline for predicting myocardial tissue remodeling and fibrosis using cardiac ultrasound. *EBioMedicine*. 2020;54:102726. doi:10.1016/j.ebiom.2020.102726
19. Han F, Wang J, Ding L, et al. Tissue engineering and regenerative medicine: achievements, future, and sustainability in Asia. *Front Bioeng Biotechnol*. 2020;8:83. doi:10.3389/fbioe.2020.00083
20. Kumar SA, Alonzo M, Allen SC, et al. A visible light-cross-linkable, fibrin-gelatin-based bioprinted construct with human cardiomyocytes and fibroblasts. *ACS Biomater Sci Eng*. 2019; 5(9):4551-4563. doi:10.1021/acsbiomaterials.9b00505
21. Bai H, Zhao Y, Wang C, et al. Enhanced osseointegration of three-dimensional supramolecular bioactive interface through osteoporotic microenvironment regulation. *Theranostics*. 2020; 10(11):4779-4794. doi:10.7150/thno.43736
22. Patel BB, McNamara MC, Pesquera Colom LS, et al. Recovery of encapsulated adult neural progenitor cells from microfluidic-spun hydrogel fibers enhances proliferation and neuronal differentiation. *ACS Omega*. 2020;5(14):7910-7918. doi:10.1021/acsoomega.9b04214
23. Safarova Y, Umbayev B, Hortelano G, Askarova S. Mesenchymal stem cells modifications for enhanced bone targeting and bone regeneration. *Regen Med*. 2020;15(4):1579-1594. doi:10.2217/rme-2019-0081
24. Moreno Manzano V, Mellado López M, Morera Esteve MJ, et al. Human adipose-derived mesenchymal stem cells accelerate decellularized neobladder regeneration. *Regen Biomater*. 2020; 7(2):161-169. doi:10.1093/rb/rbz049
25. Wong SW, Lenzini S, Cooper MH, Mooney DJ, Shin JW. Soft extracellular matrix enhances inflammatory activation of mesenchymal stromal cells to induce monocyte production and trafficking. *Sci Adv*. 2020;6(15):eaaw0158. doi:10.1126/sciadv.aaw0158
26. Radvar E, Shi Y, Grasso S, et al. Magnetic field-induced alignment of nanofibrous supramolecular membranes: a molecular design approach to create tissue-like biomaterials. *ACS Appl Mater Interfaces*. 2020;12(20):22661-22672. doi:10.1021/acsaami.0c05191
27. Lienemann PS, Martin QV, Papageorgiou P, et al. Smart hydrogels for the augmentation of bone regeneration by endogenous mesenchymal progenitor cell recruitment. *Adv sci (Wein)*. 2020; 7(7):1903395. doi:10.1002/advs.201903395
28. Begum R, Perriman AW, Su B, Scarpa F, Kafienah W. Chondroinduction of mesenchymal stem cells on cellulose-silk composite nanofibrous substrates: the role of substrate elasticity. *Front Bioeng Biotechnol*. 2020;8:197. doi:10.3389/fbioe.2020.00197
29. Sun L, Zhang S, Zhang J, Wang N, Liu W, Wang W. Fenton reaction-initiated formation of biocompatible injectable hydrogels for cell encapsulation. *J Materials Chemistry. B*. 2013;1: 3932-3939. doi:10.1039/c3tb20553c
30. Radwan IA, Rady D, Abbass MMS, et al. Induced pluripotent stem cells in dental and nondental tissue regeneration: a review of an unexploited potential. *Stem Cells Int*. 2020;2020:1941629. doi:10.1155/2020/1941629
31. Xu B, Ye J, Yuan FZ, et al. Advances of stem cell-laden hydrogels with biomimetic microenvironment for osteochondral repair. *Front Bioeng Biotechnol*. 2020;8:247. doi:10.3389/fbioe.2020.00247

32. Tang Y. Modification of bone marrow stem cells for homing and survival during cerebral ischemia. *Bone Marrow Stem Cell Therapy for Stroke*. 2016;201-239. doi:10.1007/978-981-10-2929-5_9
33. Deepthi S, Abdul Gafoor AA, Sivashanmugam A, Nair SV, Jayakumar R. Nanostrontium ranelate incorporated injectable hydrogel enhanced matrix production supporting chondrogenesis *in vitro*. *J Mater Chem B*. 2016;4 (23):4092-4103. doi:10.1039/c6tb00684a
34. Lü S, Bai X, Liu H, et al. An injectable and self-healing hydrogel with covalent cross-linking *in vivo* for cranial bone repair. *J Mater Chem B*. 2017;5:3739-3748. doi:10.1039/c7tb00776 k
35. Wu G, Feng C, Hui G, et al. Improving the osteogenesis of rat mesenchymal stem cells by chitosan-based-microRNA nanoparticles. *Carbohydr Polym*. 2016;138:49-58. doi:10.1016/j.carbpol.2015.11.044
36. Wu Y, Wang L, Guo B, X Ma P. Injectable biodegradable hydrogels and microgels based on methacrylated poly(ethylene glycol)-co-poly(glycerol sebacate) multi-block copolymers: synthesis, characterization, and cell encapsulation. *J Mater Chem B*. 2014;2(23):3674-3685. doi:10.1039/c3tb21716 g
37. Ferrigno B, Bordett R, Duraisamy N, et al. Bioactive polymeric materials and electrical stimulation strategies for musculoskeletal tissue repair and regeneration. *Bioact Mater*. 2020;5(3):468-485. doi:10.1016/j.bioactmat.2020.03.010
38. Yesildag C, Bartsch C, Lensen MC. Micropatterning of Au NPs on PEG hydrogels using different silanes to control cell adhesion on the nanocomposites. *ACS Omega*. 2018;3(7):7214-7223. doi:10.1021/acsomega.8b00863
39. Dang LH, Nguyen TH, Tran HLB, Doan VN, Tran NQ. Injectable nanocurcumin-formulated chitosan-g-pluronic hydrogel exhibiting a great potential for burn treatment. *J Healthcare Eng*. 2018;2018:5754890. doi:10.1155/2018/5754890
40. Du X, Zhou J, Shi J, Xu B. Supramolecular hydrogelators and hydrogels: from soft matter to molecular biomaterials. *Chem Rev*. 2015;115(24):13165-13307. doi:10.1021/acs.chemrev.5b00299
41. Huang CL, Chen YB, Lo YL, Lin YH. Development of chitosan/ β -glycerophosphate/glycerol hydrogel as a thermosensitive coupling agent. *Carbohydr Polym*. 2016;147:409-414. doi:10.1016/j.carbpol.2016.04.028
42. Zhang W, Jin X, Li H, Zhang R, Wu C. Injectable and body temperature sensitive hydrogels based on chitosan and hyaluronic acid for pH sensitive drug release. *Carbohydr Polym*. 2018;186:82-90. doi:10.1016/j.carbpol.2018.01.008
43. Ramírez Barragán CA, Macías Balleza ER, Uriostegui LG, Andrade Ortega JA, Toriz G, Delgado E. Rheological characterization of new thermosensitive hydrogels formed by chitosan, glycerophosphate, and phosphorylated β -cyclodextrin. *Carbohydr Polym*. 2018;201:471-481. doi:10.1016/j.carbpol.2018.08.076
44. Assaad E, Maire M, Lerouge S. Injectable thermosensitive chitosan hydrogels with controlled gelation kinetics and enhanced mechanical resistance. *Carbohydr Polym*. 2015;130:87-96. doi:10.1016/j.carbpol.2015.04.063
45. Yu S, Zhang X, Tan G, et al. A novel pH-induced thermosensitive hydrogel composed of carboxymethyl chitosan and poloxamer cross-linked by glutaraldehyde for ophthalmic drug delivery. *Carbohydr Polym*. 2017;155:208-217. doi:10.1016/j.carbpol.2016.08.073
46. Jommanee N, Chanthad C, Manokruang K. Preparation of injectable hydrogels from temperature and pH responsive grafted chitosan with tuned gelation temperature suitable for tumor acidic environment. *Carbohydr Polym*. 2018;198:486-494. doi:10.1016/j.carbpol.2018.06.099
47. Viezzer C, Mazzuca R, Machado DC, de Camargo Forte MM, Gómez Ribelles JL. A new waterborne chitosan-based polyurethane hydrogel as a vehicle to transplant bone marrow mesenchymal cells improved wound healing of ulcers in a diabetic rat model. *Carbohydr Polym*. 2020;231:115734. doi:10.1016/j.carbpol.2019.115734
48. Ressler A, Rochina JR, Ivanković M, Ivankovi H, Rogina A, Ferrer GG. Injectable chitosan-hydroxyapatite hydrogels promote the osteogenic differentiation of mesenchymal stem cells. *Carbohydr Polym*. 2018;197:469-477. doi:10.1016/j.carbpol.2018.06.029
49. Yen CH, Li ST, Cheng NC, Ji YR, Wang JH, Young TH. Label-free platform on pH-responsive chitosan: adhesive heterogeneity for cancer stem-like cell isolation from A549 cells via integrin β 4. *Carbohydr Polym*. 2020;239:116168. doi:10.1016/j.carbpol.2020.116168
50. Dong Y, Liang J, Cui Y, Xu S, Zhao N. Fabrication of novel bioactive hydroxyapatite-chitosan-silica hybrid scaffolds: combined the sol-gel method with 3D plotting technique. *Carbohydr Polym*. 2018;197:183-193. doi:10.1016/j.carbpol.2018.05.086
51. Takei MN, Kuda T, Taniguchi M, Nakamura S, Hajime T, Kimura B. Detection and isolation of low molecular weight alginate- and laminaran-susceptible gut indigenous bacteria from ICR mice. *Carbohydr Polym*. 2020;238:116205. doi:10.1016/j.carbpol.2020.116205
52. Kumar R, Rahman H, Ranwa S, Kumar A, Kumar G. Development of cost effective metal oxide semiconductor based gas sensor over flexible chitosan/PVP blended polymeric substrate. *Carbohydr Polym*. 2020;239:116213. doi:10.1016/j.carbpol.2020.116213